Development of the Electrodeless Plasma Thruster at High Power: Investigations on the Microwave-Plasma Coupling

IEPC-2007-240

Presented at the 30th International Electric Propulsion Conference, Florence, Italy
September 17-20, 2007

Gregory D. Emsellem*
The Elwing Company, Wilmington, DE, 19801, USA

and

Serge Larigaldie†
ONERA - Office National d'Etude et Recherche Aéronautique, Palaiseau, 91120, France

Abstract: Improving the performances of the Electrodeless Plasma Thruster at higher power level requires gaining a deeper understanding of the microwave-plasma energy coupling. In order to investigate in details the dynamic of this coupling and its variations under diverse operational conditions, the Elwing Company has developed specific, highly versatile, components that can be fitted on the current 8-12 kW model of the electrodeless plasma thruster. This article fully exposes the development process of these components, which involves finite elements modeling, along with the design characteristics and operational capabilities of the microwave applicator and the magnetic structure.

Nomenclature

B	=	magnetic field
E	=	electric field
F	=	accelerating force
I	=	electrical current intensity
I_{sp}	=	specific impulse
m	=	particle mass
m_e	=	electron mass
n	=	plasma particle density
n_e	=	plasma electron density
Ψ	=	ponderomotive potential
q	=	electrical charge of a particle
v_c	=	cyclotronic velocity of a particle in a magnetic field
ε_0	=	vacuum electrical permittivity
μ	=	adiabatic invariant or magnetic momentum of a charged particle in a magnetic field
ω	=	applied electromagnetic field pulsation or angular frequency
Ω_c	=	particle cyclotronic pulsation or angular frequency in a magnetic field
ω_p	=	plasma pulsation or angular frequency

* Chief Scientist, Elwing R&D Departement., research@elwingcorp.com.
† Senior Research Engineer, Office National d'Etude et Recherche Aéronautique (ONERA), DMPH / DOP, serge.larigaldie@onera.fr.

I. Introduction

PRODUCING large amounts of thrust with electric propulsion devices, without increasing the physical dimensions of a thruster, requires the ability to accelerate efficiently dense plasma beams. Indeed, accelerating plasma by a magnetized ponderomotive force field allows, in theory, the efficiency of this process not to be affected by the plasma density, such an independence being shared only with acceleration by Lorentz force as in MagnetoPlasmaDynamic (MPD)/Lorentz Force Accelerator (LFA) or Pulsed Inductive (PIT) thrusters. In turn, this possibility could initiate the use of electric propulsion devices for energetic manoeuvers currently achievable only by chemical propulsion or lower-specific impulse electrothermal devices.

Nevertheless, from a practical point of view, to remain efficient, this acceleration process should not be disturbed by external factors such as microwave field pattern modifications in resonant cavity by plasma loading effect. For more than 30 years, numerous studies have been conducted on microwave-excited plasma[1], in general, and more specifically on Electron Cyclotron Resonance (ECR) plasma[2]. Even more work has been dedicated to understanding the behavior of loaded microwave cavities at high power, especially for heating applications[3]. However, it remains that producing ECR plasma in a non-uniform magnetic field inside a single-mode resonant cavity has never been studied from an experimental or numerical point of view. This is even truer when the microwave field is used to generate a ponderomotive force field.

Hence, the Elwing Company felt the need to explore, both numerically and experimentally, the microwave-plasma coupling in the electrodeless plasma thruster. The ability to measure the global impedance of the plasma beam for various operational conditions (mass flow rate, applied power, power balance, propellant gas) provide both a deeper understanding of the microwave-plasma interaction as well as a mean to accurately design complex cavities optimized for specific operational regimes. These capabilities are all the more important at higher power, as the microwave power not coupled to the plasma is dissipated in the microwave circuit generating potentially large heat loads.

This article exposes the rationale of and the results obtained during the conception of the four generations of microwave applicators developed to date, with a special emphasis on the broadly tunable cavity developed with the special purpose of investigating the microwave-plasma interactions. Lastly, ECR in both ionization and acceleration stage of the electrodeless plasma thruster not only depends on the microwave field but also on the magnetic field topology. Thus, this article also explains in details the rationale and results of the designing process of the thirteen magnetic structures studied. Both finite elements simulated and experimentally measured 3D electromagnetic fields are presented for the retained structure.

II. High Power Challenges and Electrodeless Plasma Thruster Rationale

For the past five years, the Elwing Company has developed the electrodeless plasma thruster concept to leverage the plasma density independence of the ponderomotive force acceleration. Before explaining in details the objectives, methods employed and the resulting sub-systems, we will begin by reviewing the electrodeless plasma thruster principle and basic setup.

The basic concept has been evolved toward both lower and higher power thruster than commercially available units, roughly between 1 to 5kW. Both these R&D ventures requires dedicating significant efforts to optimize the power coupling : at low power to insure the device remains efficient enough to be worth using, while at high power to minimize the thermal loads generated by power losses.

A. The Magnetized Pondermotive Force

The ponderomotive force is created by a gradient of electromagnetic (EM) energy density[1]. For a non-magnetized plasma, using plasma frequency (Eq. (2)), this force is directly proportional to the gradient in Eq. (1)

$$\vec{F} = -\frac{\omega_p^2}{2\omega^2}\vec{\nabla}\frac{\varepsilon_0 E^2}{2} \tag{1}$$

$$\omega_p^2 = \frac{n_e e^2}{m\varepsilon_0} \tag{2}$$

From Eq. (1), one can notice that the intensity of this force actually increase as the square of plasma density, while it decrease with higher EM frequency. These effects mean that the ponderomotive force is stronger in dense plasma submitted to low frequency electromagnetic fields. Nevertheless, the benefits of lowering the frequency should be balanced by the fact that as the plasma density increase low frequency fields tends to be shielded out.

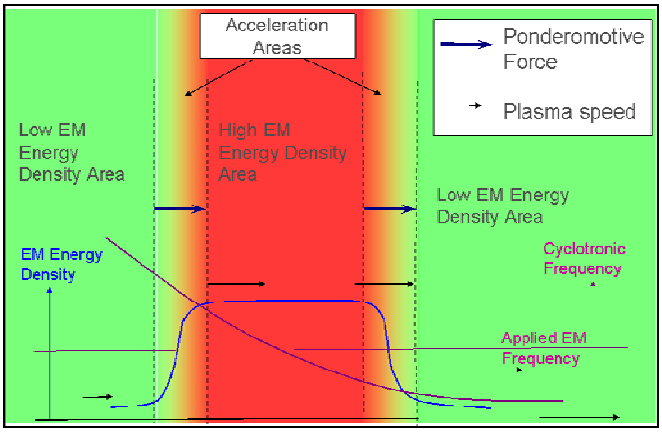

Figure 1. Schematic field topology of magnetized ponderomotive force field created by a high energy density area on a decreasing static magnetic field. *The reversal of the sign of the difference between applied field frequency and local cyclotron frequency allows the magnetized ponderomotive force to have the same direction on both areas of electromagnetic energy density gradients.*

The presence of a static magnetic field strongly modifies the ponderomotive force as described in Eq. (3). While the first part closely resemble the unmagnetized force, only modified by apparition of the difference between the local cyclotronic frequency (Eq. (4)) and the frequency of the applied electromagnetic field, two other terms appears that have no equivalent in the unmagnetized situation.

One of these new terms is similar to the so-called "μ-grad B" force existing in non-uniform magnetic field and the other term is proportional to both magnetic field gradient and electromagnetic energy density. We will just notice that the magnitude of the "μ-grad B" force is smaller than the other terms and that the other term is significant only in the close vicinity of the resonance.

$$\vec{F}_{magnetized} = -\frac{\omega_p^2}{2\omega(\omega-\Omega_c)}\vec{\nabla}\frac{\varepsilon_0 E^2}{2} - \frac{\omega_p^2}{2\omega(\omega-\Omega_c)^2}\frac{\varepsilon_0 E^2}{2}\vec{\nabla}\Omega_c - \mu\vec{\nabla}B \tag{3}$$

$$\text{With } \Omega_c = \frac{qB}{m} \tag{4}$$

An interesting effect of the magnetic field modification of the ponderomotive force is the possibility to reverse the direction of the force, when the local magnetic field is larger than the resonant field (B_{res}).Such magnetized ponderomotive force can be used to create (as in Fig. 1) a succession of accelerating force fields, all aligned in the same accelerating direction. The electrodeless plasma thruster is based on this effect to accelerate a plasma beam.

B. The Electrodeless Plasma Thruster Structure Rationale

The idea behind the Electrodeless Plasma Thruster is to accelerate the plasma by applying a strong and non-uniform EM Field in an area of static magnetic field decreasing along the thrust axis. Hence, the design of an efficient electrodeless plasma thruster consists of solving three problems:

- The first one is to efficiently produce a dense and cold plasma,
- The second to produce a strong accelerating magnetized ponderomotive field
- Last, these structures need to be efficiently coupled so the plasma can flow smoothly between the ionization and the acceleration area.

Of course, all these problems are quite complex and, in fact, dependent from each other. Furthermore, designing an electrodeless plasma thruster presents a special challenge, as the dimensioning of the device is not directly linked to the nominal power or the thrust level of the thruster but rather by the operating frequency of the acceleration structure.

The accelerating magnetized ponderomotive field is composed, as exposed above, of three added vector fields.

The easiest to understand is the "μ-grad B" part, which, aside from any cyclotronic heating effects, depends only of the magnetic field value between the place where the plasma particle are created in the ionization area and at the exit of the thruster. This field does not require any specific optimization as the only parameter is the magnetic field value in the ionization area.

The part which resemble to unmagnetized ponderomotive force is the most important one in intensity and effects and requires steep EM energy density gradient, ideally with the local cyclotronic frequency as close as possible to the applied EM frequency, and of course a magnetic field higher than the resonant field on the upstream gradient.

The component of the force field is only noticeable near the resonance area and at this point requires a high EM energy and magnetic field gradient. This last force field component, even if less important, is difficult to optimize because a lower magnetic field gradient create a larger acceleration area around the resonance but in the same time reduce the magnitude of this accelerating force. Last, but not least, as the accelerating force is directed along the EM and magnetic fields gradients, these gradients should be aligned with the thrust axis to limit the beam divergence.

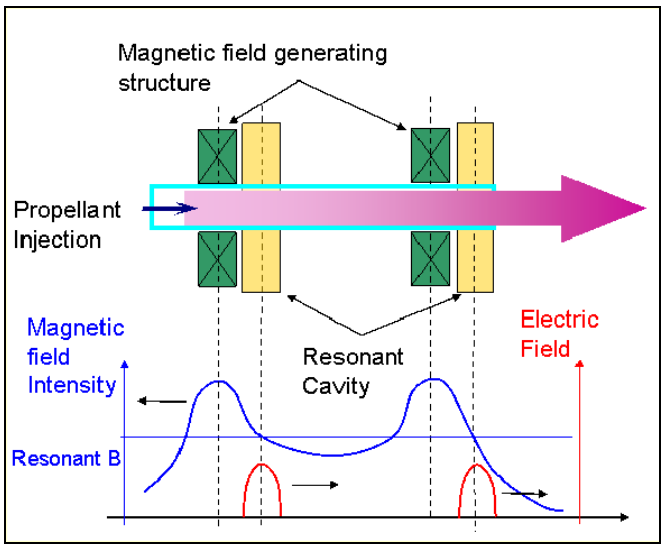

Figure 2. Overview of the fields' topologies in the electrodeless plasma thruster. *The magnetic structure creates an axial magnetic field featuring a magnetic bottle and a diverging field suitable for ponderomotive force. The resonators create the localized EM field with steep gradients adapted to ponderomotive force acceleration.*

Hence, these various and partially opposing constraints define an optimal topology comprising an area of localized high EM energy density with steep "sides" on a steadily decreasing magnetic field "slope". This topology can be created by using a simple metallic hollow resonator located downstream from a coil as represented in Fig. 2 near the exit of the thruster (right half of the thruster).

The constraints on the ionization part of the thruster can be summarized as focused on ionization efficiency, the ability to produce dense and cold plasma, durability and compatibility with the strong magnetic field required upstream of the acceleration area. This last constraint actually was turned into strength. Indeed, the presence of a static magnetic does improve the efficiency of most ionization mechanism, at the very least due to the ability of magnetic field to limit electron diffusion across magnetic field lines. Furthermore, applying a magnetic field allows ionizing gas by one of the numerous resonances that do not exist in unmagnetized plasma.

Following this idea, it appears that wave driven ionization stage present the additional benefit of being electrodeless, hence, intrinsically durable and rugged. The most efficient ionization electrodeless structure appears to be the electron cyclotron resonance ECR. This is quite an ironic fact as modern ECR plasma sources do indeed stem from the researches conducted to develop ponderomotive force driven "plasma injector". In order to further enhance the ECR source efficiency, we imagined that, instead of applying a uniform magnetic field, we could set the ECR area between two magnetic field maxima hence creating a "leaking magnetic bottle", and use a resonator as applicator of the ECR EM field. Adding this special ECR source upstream of the ponderomotive accelerating stage seems the best option that did gave birth to the structure exposed illustrated Fig.(2). Using an ECR ionization stage allows using the same frequency, thus the same EM wave source, for feeding EM energy to both stages.

One could notice here that while both ECR and non-ECR microwave plasma sources have been thoroughly studied over almost three decades, we have not found any reference to an ECR arrangement using a magnetic bottle and a cavity resonator applicator. This might be the results of researches focused on either well confined source producing highly charged ions (at low density) for particle accelerator or on source producing large volume of chemically reactive plasma, where plasma confinement is not an important factor compared to plasma homogeneity.

This basic scheme, which features several advantages (erosion free, efficient, compact, throttleable), can be applied to produce electrodeless plasma thruster of any nominal power or thrust. This scheme needs only to be scaled with the frequency of the EM power. Furthermore, whereas this scheme is exposed above in a simple cylindrical geometry, it can be adapted to different geometries such as polygonal or concentric.

This concept can be adapted to use a wide range of frequency. Selecting the nominal frequency impose a minimal size for the device and an overall minimal value of the magnetic field. Besides, the structure can be broadly modified as it can incorporate many different magnetic assemblies (combining coils, electromagnets and permanent magnets) and many different EM power circuits and applicators.

The 2.45GHz ISM frequency present many advantages including availability of highly efficient power generators (at a broad range of nominal power from a few Watts up to many KiloWatts) and availability of extensive research results on using this frequency for plasma interaction.

The high power electrodeless plasma thruster prototype uses microwaves at this frequency. The resonant magnetic field intensity corresponding to this frequency can be created by permanent magnet assembly. Hence, our team decided that the magnetic field would be generated by a permanent magnet assembly using advanced permanent magnet material.

C. High Power Challenges of the Electrodeless Plasma Thruster

The high power Electrodeless Plasma thruster was conceived to operate at nominal power up to 20 kW, and more specifically in a regime of higher thrust. The same device can indeed be operated at lower power, yet the basic scheme can be differently optimized for lower power operation focusing more on reducing mass, size and complexity.

The main challenge in high-power/high-thrust regime consists of heat loads that might be difficult to manage. These heat loads are due to a few basic causes: surface currents in the microwave structure, high-energy plasma particles impingement on the structure, to a lesser extent radiation from the plasma. Obviously, these heat loads can be diverted and/or radiated away by heat management structure. Nevertheless, limiting the heat produced at their sources seems better than simply removing it. Besides, even if the overall temperature of the thruster structure could certainly be kept steady, it might be quite elevated in some locations or components, this is especially true when using advanced permanent magnets, which loose their magnetization when exposed to high temperature.

The radiation heating cannot be fully suppressed, only controlled, mainly by keeping the plasma cold before it reaches the acceleration stage. While the microwave applicators are not affected at all by the radiative heating the magnetic assembly can easily be shielded from it.

The particle impingement on the structure is also strongly reduced if the plasma upstream from the acceleration stage has a low temperature. This particle flux can be further reduced by magnetic mirror effect with adequate magnetic field topology.

The most difficult to handle heating source is microwave losses because it fundamentally depends of the plasma-wave coupling. This coupling depends on plasma density and both microwave and static magnetic field topologies. After reviewing numerous papers, our opinion is that a large part of the knowledge on ECR coupling is empirical. Whereas ECR coupling has been studied extensively in numerous publications, most analytical models are based on extremely simplified assumptions. Therefore, these analytical models are not accurate enough to predict the coupling parameters to design optimized applicator in case where both the magnetic field and the applied microwave fields are non-uniform over small scales.

High-power/high-thrust operations can also be affected by plasma shielding effects. Dense plasma can behave like a good conductor and both absorb and reflect a significant part of the microwave energy resulting in a field that cannot reach the deeper part of the plasma beam. This effect is reduced by the static magnetic field; it can be further limited by carefully designed magnetic field topology.

These challenges can best be overcome by working on the magnetic and microwave field topologies. In consequence, the development of advanced magnetic generating structure and microwave applicator needed to be focus of dedicated efforts. Moreover, these structures needed to be versatile to allow experimental measurement of the actual coupling parameters under various operational conditions. These measured parameters will allow gaining a deeper understanding of the physics of this coupling resulting in the development of accurate analytical models.

The next section will review the work done by the authors on the magnetic and microwave structures.

III. Development of the High Power Electrodeless Plasma Thruster

The previous section outlined the necessity to develop advanced microwave applicators and magnetic structure for the High Power Electrodeless Plasma Thruster.

This section will first review the development process of the four generations of microwave applicators, from the constraint and objectives to the actual applicator design. Similarly, the second part of this section depicts the same process for the magnetic assembly where most of the thirteen major version of this structure will be exposed.

A. High Power Microwave Structure Development

The microwave applicators have a crucial importance in the operation of Electrodeless Plasma Thruster, even more so at high power operation. We will first summarize the objectives and methods of the development, and later expose the various configurations and detail the produced field.

1. Aim and Methods of Microwave Applicators Developments

The microwave applicators create the essential stationary non-uniform microwave fields to ionize the propellant and accelerate the plasma. Both of these stages must be optimized to insure efficient plasma-microwave coupling. Whereas both applicators operate at the same frequency and field polarization, their different purposes imply that their optimized coupling parameters are quite different in the ionization and in the acceleration stage.

Applicators development target

The ionization cavity should produce ionize the propellant to produce a dense and cold plasma in a leaky magnetic bottle, it is almost a regular ECR source. This function requires smoothly accelerating the free electrons to

ionize the neutral propellant atoms; it can be performed by supplying a moderate field intensity in where the magnetic field reach the resonant value, the energy density gradients are not important. The plasma inside this cavity will be quite dense and cold, the magnetic field topology around this cavity will be a magnetic bottle.

The accelerating cavity must create a stationary wave field featuring a very high maximum energy density in the resonance area and with steep gradients along the thruster axis. The plasma inside this cavity will be strongly heterogeneous (a variation of two order of magnitude of the density between the upstream and downstream sides of the cavity) on a decreasing magnetic field. The power flowing through this cavity can be up to one order of magnitude larger than in the ionization cavity.

These cavities must nevertheless achieve partially similar goal: creating stationary microwave field with a maximum on the thruster axis and a polarization orthogonal to this axis. The stationary microwave field should ideally be setup in a mode such that the variation of the plasma load does not affect the overall field pattern. They must also satisfy a host of practical requirements including being fed by waveguides, fitting inside the magnetic and mechanical structure, being highly conductive, non-magnetic, small and light, and, most importantly, accommodate the 6 cm wide opening through which the plasma flow along the thruster axis.

Beyond all these requirements, these cavities must be able to permit the measurement of the plasma impedance at least from back modeling. The determination of plasma impedance in each cavity for any given set of operational parameters being the key objective of this experimental investigation.

Applicator design evaluation methodology

The design process consisted of seven steps of simulations, using commercial Finite Element Analysis package.

1- Applicator propagation properties study in free space – This essential step proof that the structure does allow the microwave power to reach every part of the not closed applicator. It also ensures the resonator does not produce strong reflection in the feeding circuit.
2- Applicator resonance study – This step permit the evaluation of the natural resonance frequency of the applicator in absence of any plasma load. Moreover, this step eliminates geometries that present a natural resonance in which the steady field would present a polarization along the thruster axis.
3- Applicator system resonance study – this study confirmed the influence of the external tuning elements on the resonance mode inside the applicator. This study also allows evaluating the magnitude of the influence of this external tuning element.
4- Study of the applicator system in ionization stage and acceleration stage on vacuum – This step evaluates the effects of the rest of the thruster structure on the behavior of the applicator system.
5- Study of the applicator system in ionization stage and acceleration stage in vacuum tank – Checking that the applicator systems are not affected by facility effect (for small metallic vacuum chambers)
6- Study of the applicator system loaded with a simple homogeneous resistive non-resonant plasma – This step simply evaluate the actual field pattern modification and impedance modification create by « simple » resistive plasma of given densities.
7- Study of both applicator systems on the thruster in vacuum tank – This step was performed solely to evaluate the cross talk between cavities.

At each of these steps, impedance response and resonance frequencies as well as field topology and field polarization were gathered. Starting at Step 4 the surface current field was also examined to localize potential difficulties. It should also be noted that in most of these simulation the applicator system was evaluated by modeling its response to a Gaussian waveform of variable frequency width.

2. Applicator development process and results

For each of the four applicator shapes "family", many different geometrical parameters (such as height, width, radius, length along the thruster axis, etc…) were tested according to the methodology described above, resulting in more than half a thousand simulations over the course of three years. Obviously, not all these results could be described in this article, consequently, after presenting each of the four shape families, we will present key results for the most versatile applicator developed.

Applicator design families

Four basic applicator designed have been developed to date, each with their own strengths and weaknesses. They all could be efficiently used on an Electrodeless Plasma thruster either in the ionization or in the acceleration stage.

The first applicator design considered was the simplest, a cylindrical cavity coupled to a waveguide by an aperture (Fig. 3). This design has the advantages of simplicity, compactness and reduced weight. Its main drawbacks are its microwave field pattern low sensitivity to alteration by external tuners, and high sensitivity to alteration by plasma load variation. Last, the geometrical parameter of this applicator cannot be easily modified. Such cylindrical applicator can nonetheless produce suitable field pattern as illustrated in Fig. 4.

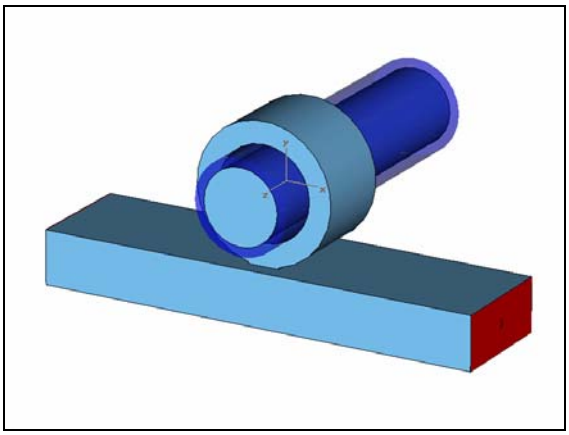

Figure 3. Overview of the cylindrical applicator geometry. *The cylindrical applicator is coupled to the feed waveguide below by an aperture. The dark blue cylinder represents the quartz tube surrounding the thruster chamber.*

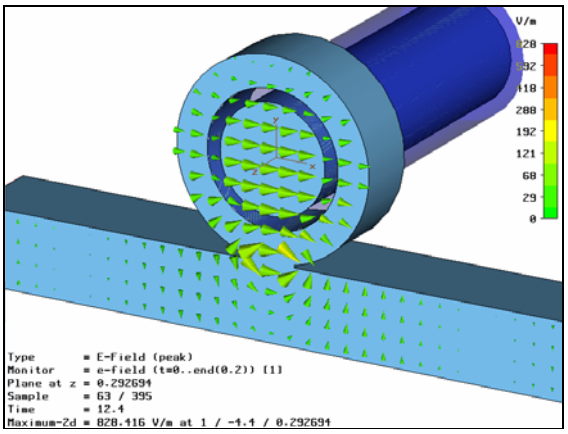

Figure 4. Field pattern in the middle plane of the cylindrical applicator. *The field pattern inside the cylindrical applicator, represented by the colored arrows, is clearly polarized horizontally and strong on the thruster axis.*

The following applicator structure to be developed is also cylindrical but concentric as it comprise an annular cavity around the central cylindrical cavity where the plasma chamber is located (Fig. 5). This annular cavity destroys the reciprocity[‡] of the basic cylindrical structure. This is a great advantage because we want the field pattern to remain unaffected by changes in plasma impedance and nonetheless to be affected by external tuner adjustments'. Moreover, the annular cavity, and position of the coupling apertures, can act as a mode filter, which can prevent undesired mode from appearing independently from any variation in the plasma impedance, hence really defining the mode. The disadvantage of this structure is the fact that it offers less tuning capability than the other geometries (one cannot build a variable radius concentric cavity.). This concentric applicator offers ideal field pattern (Fig. 6) when designed for well-defined load impedance.

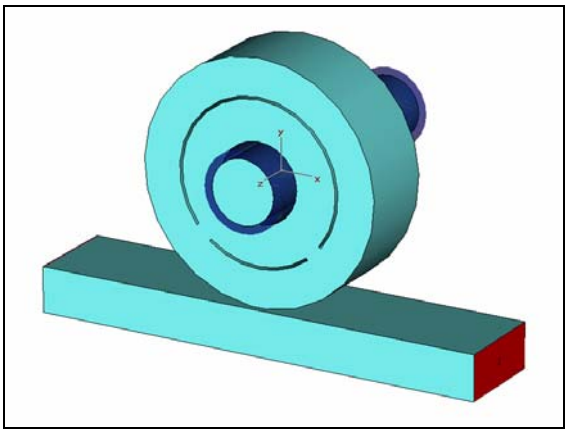

Figure 5. Overview of the concentric applicator geometry. *The wall separating the annular from the cylindrical part of the applicator is clearly visible. The two interruptions in this wall are the coupling apertures.*

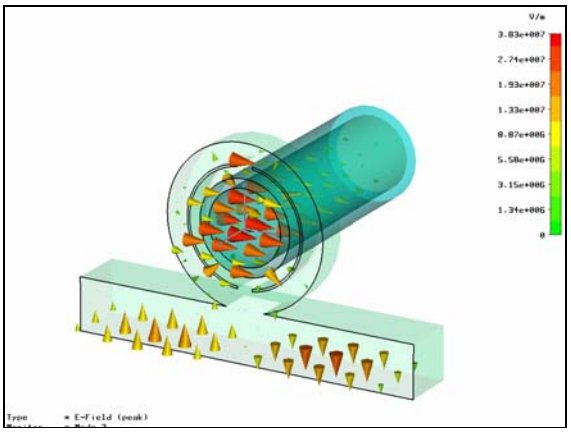

Figure 6. Field pattern in a concentric applicator. *The two coupling apertures are located 180° apart in this concentric configuration. The high value and horizontal polarization of the field on the thruster axis is noticeable.*

A third applicator design has been derived from a rectangular resonator. Because rectangular cavities analytical approach is straightforward, the back-evaluation of the plasma impedance is greatly simplified. The resulting geometry is surprisingly complex (Fig. 7 & Fig. 8). Whereas the central section of the applicator is a rectangular brick through which the plasma chamber goes through, it is surrounded on both sides by truncated tetrahedron allowing smooth transition between the waveguides and the central section. The resulting shape somehow resembles a hammerhead. The waveguide usually has both a smaller height (along the vertical axis) and a larger depth (along the thruster axis) than the applicator central section.

This complex geometry presents the ability to modify the effective width of the applicator (horizontal direction orthogonal to thruster axis). It also features more geometrical parameters than the previous geometries, especially the transition area width. Therefore, this geometry benefits of wider impedance adjustments capabilities and seems not reciprocal. The disadvantages of this structure are its important width, mechanical complexity and larger weight. All the figure of merits of this structure are excellent. The details of the microwave structure will be the one exposed in details in the next part of this section

[‡] The reciprocity of a microwave structure is the fact that the impedance between two ports is the same regardless of the direction of the wave motion through the structure. Another explanation is that a structure is symmetrical if the impedance viewed from each port is the same.

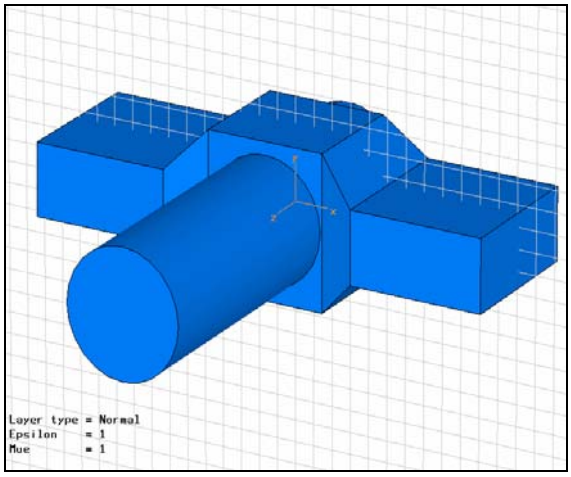

Figure 7. Perspective view of the geometry of the "hammerhead" applicator. *Two waveguide sections are visible on each side of the applicator. The left one is feeding power to the cavity whereas the right one is just a short circuit.*

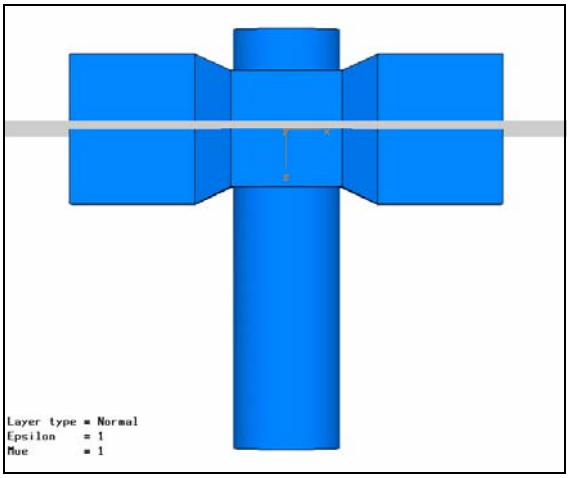

Figure 8. Top view of the geometry of the "hammerhead" applicator. *The central section traversed by the thruster chamber is clearly less deep than the feeding waveguides on both sides.*

The fourth geometry developed is a special version of the well-known and efficient "downstream source" (Fig. 9 & Fig. 10). Usually these plasma sources are composed of a short-circuited waveguide wherein a plasma-containing tube is positioned across the wider cavity wall around a maximum of the electric field. For the sake of clarity, we want to precise that traditional downstream source do not involve ECR or magnetic field, incidentally this can be guessed by the fact that this basic geometry apply a microwave electric field aligned along the plasma tube axis.

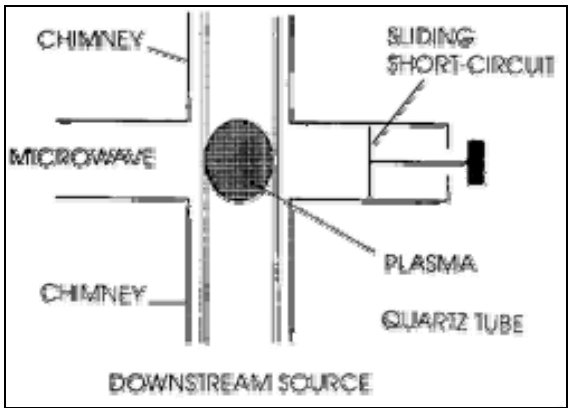

Figure 9. Schematic representation of a traditional downstream applicator. *The sliding short circuit on the right allows keeping the field maximum despite the plasma permittivity.*

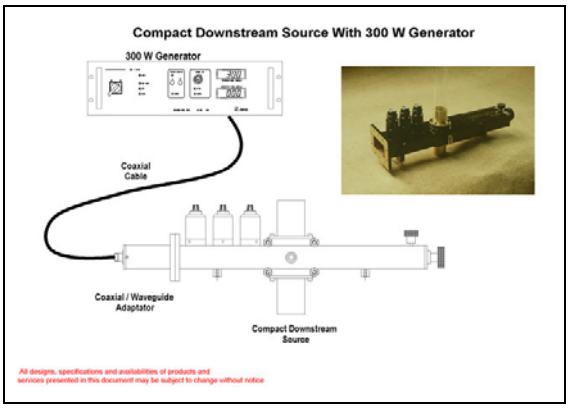

Figure 10. Microwave downstream plasma source circuit diagram. *The picture inset represents an advanced commercial downstream applicator featuring additional stub tuner. (Courtesy of SAIREM SA, France © all rights reserved.)*

The idea of this development[§] is to position the plasma tube through the cavity smaller wall (Fig. 11), thus the field gradients along the plasma tube axis are steeper and the electric microwave field become orthogonal to the plasma tube axis thus suitable for ECR coupling. This structure features all the same advantages as the hammerhead applicator plus greater versatility and mechanically simplicity. The disadvantage of this concept resides in its heavier weight. As can be noticed in the Fig. 12, the field topology fulfills the functional requirements.

[§] This brilliant idea was suggested by a one of our partners listed in the acknowledgments section.

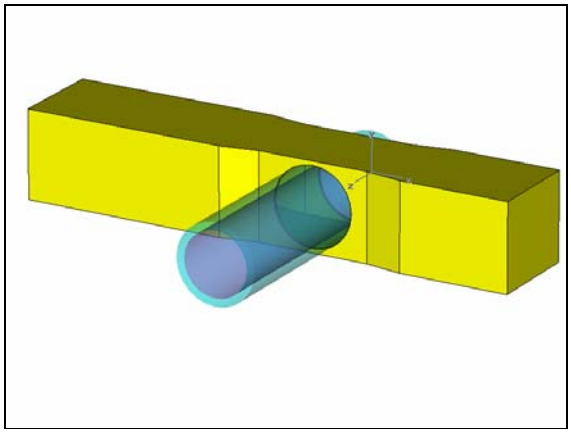

Figure 10. Top view of the geometry of the "downstream-type" applicator. *In this example, the central section around the thruster chamber is slight depressed.*

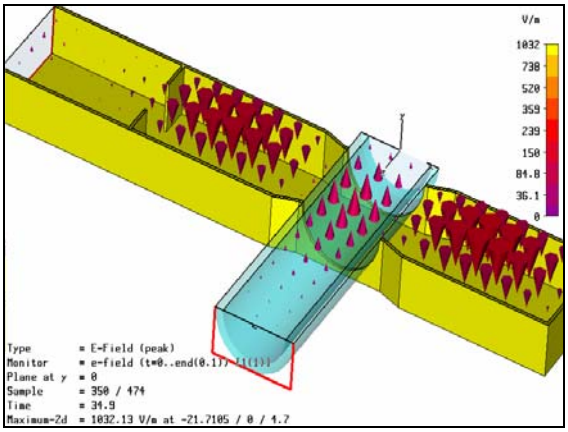

Figure 11. Electric field pattern in the "downstream-type" applicator. *The adjustable iris is clearly visible on the left side of the applicator.*

Before reviewing results obtained during the elaboration of the "hammerhead" type applicator, we want to stress the fact that these simulation results surprisingly proved all these structures could be efficiently used in the electrodeless plasma thruster at high power. The selection of the actual structure used in the high power prototype was based on their ability to apply the same filed pattern to broadly different plasma loads and easiness to derive the actual plasma impedance from the tuner setting.

« Hammerhead » applicator detailed development results.

The first step of the design process is the evaluation of the propagation characteristics of this applicator. Specifically three amplitude ratio are examined, these ratio are usually measured in dB and measure the power exiting a given port divided by the power entering either a different port (transmission parameter) or the same port (reflection parameter).

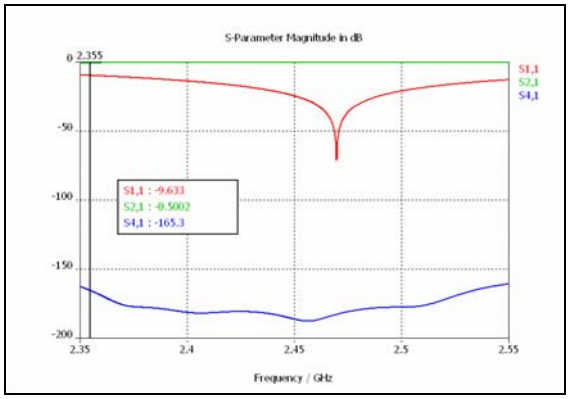

Figure 12. Frequency response of the "hammerhead" applicator. *The reflection coefficient (red line) presents a minimum below -70dB around 2.47GHz.*

The power entrance reflection coefficient, called S_{11}, must be as low as possible over a wide range of frequency around the operating frequency. This large bandwidth requirement is due to microwave sources frequency instability (e.g. 2450±25 MHz for magnetron).Similarly, the power entrance to power exit transmission coefficient, S_{12}, should be as high as possible as it proves that progressive waves can move through the applicator without any obstacles. This insures that, once an adjustable short-circuit is fitted on the power exit, these waves will be able to reach it and, being properly reflected, will establish a stable stationary wave field. Last, the applicator also has two openings on the side to allow the plasma flow. The transmission coefficient from the power entry port to these apertures, S_{13} and S_{14}, must be as low as possible to prevent the microwave power from escaping through these opening instead of being confined inside the resonator.

This complicated structure, built with adequate geometry, demonstrated a considerable bandwidth (greater than 150 MHz) where all these parameters are simultaneously acceptable: as shown in Fig. 12, S_{11} is lower than -16dB, S_{12} larger than -0.3dB and S_{13} approximate value is well below -150dB between 2.4 and 2.5 GHz.

These values confirm the capabilities of this structure as an efficient microwave applicator. The low value of the S_{13} coefficient proves that regardless of the large size of the opening in the side of the cavity the energy remains undeniably confined inside the cavity.

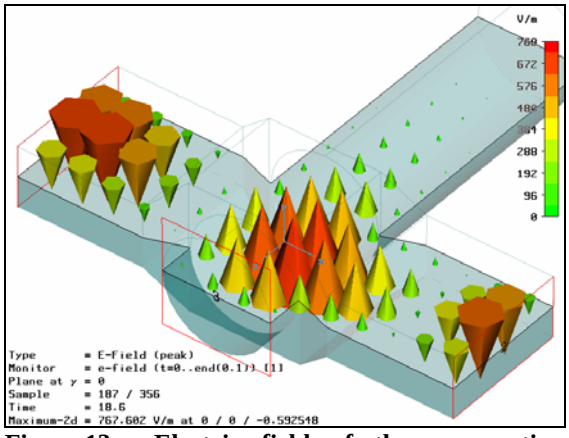

Figure 13. Electric field of the propagating wave in the horizontal plane. *Arrows represents the local electric field vector. Size and color represent relative intensity. The microwaves propagate from the upper left waveguide section to the lower right one. Field is nearly exactly vertical everywhere. The field intensity decreases along the thruster axis.*

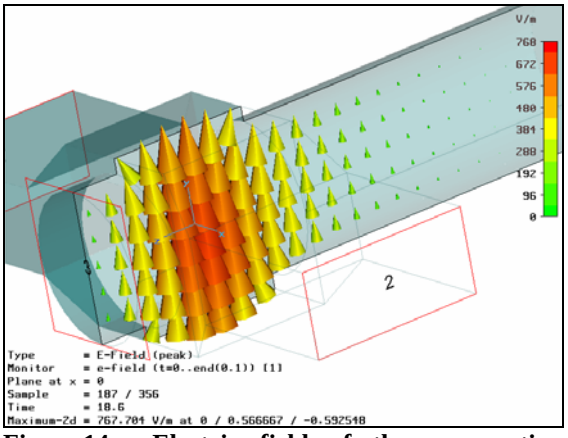

Figure 14. Electric field of the propagating wave in the vertical plane along thruster axis. *The electric field intensity sharply decreases along the thruster axis. This cut reveals small curvature of the field lines in the immediate vicinity of side apertures edges'.*

Analysis of the progressive wave topology, as they travel through this structure (Fig. 13, Fig. 14 & Fig. 15), displays that the electric field polarization remains vertical inside the applicator.

Confirming S-parameter data interpretation, graphical representations of the field intensity (Fig. 16) and energy density (Fig. 17) inside the cavity shows that the wave does not propagate outside the cavity along the thruster axis. Nonetheless, the field value is far from being negligible at the missing wall of the cavity because of the apertures. The field behaves much like a compressed soft solid; it does swell a bit through the holes but not too far. This is probably caused by the fact the thruster chamber is too small for this frequency to propagate.

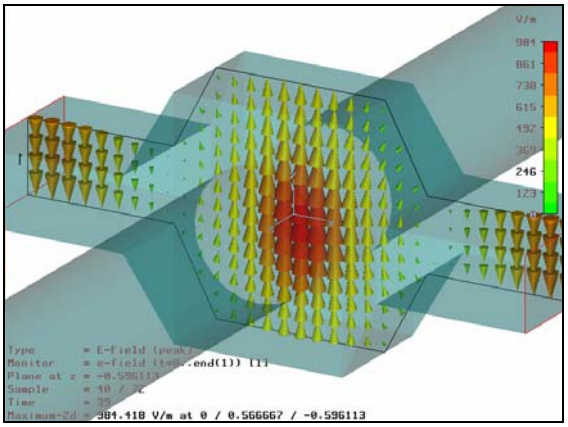

Figure 15. Electric field of the propagating wave in the vertical plane across the thruster axis. *The electric field polarization is mostly vertical only slightly curved in the transition areas. The direction of the electric field is the same in both waveguides the distance between them being roughly 3/2 of the wavelength.*

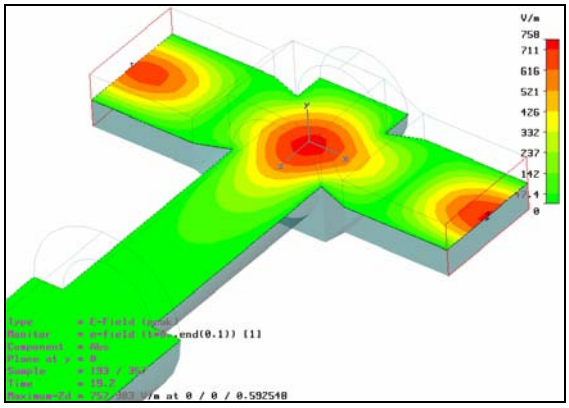

Figure 16. Electric field intensity in the horizontal plane. *Red areas notify intense local electric field. Green areas signify weak electric field. The field intensity quickly decreases along thruster axis. The applicator is positioned in the ionization stage here and the thruster connected to a small vacuum vessel.*

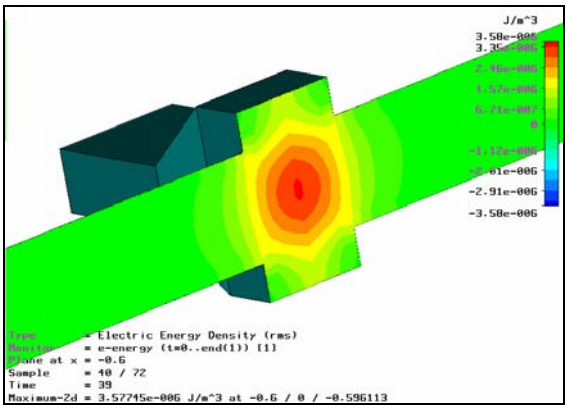

Figure 17. Microwave field energy density in the vertical plane along thruster axis. *The energy density peaks in the center of the cavity. Strong gradient are located in the plane of the applicator walls. Isolines are remarkably vertical.*

The resonance study of this applicator structure reveals the absence of any natural modes of resonance between 2.32 GHz and 2.59 GHz. Moreover, the closest natural frequencies correspond to modes where the electric field is perpendicular to the thruster axis and maximum intensity on the axis. On the opposite, when fitted with external tuning element, the applicator system can be tuned to create a stationary wave system, for any frequency comprised between 2.35GHz and 2.55 GHz and any resistive plasma density from $10^7 cm^{-3}$ to $10^{14} cm^{-3}$, with a topology mostly similar to the field presented in Fig. 13 to Fig. 17.

The later stages of the development process confirmed the capabilities of this structure with the noticeable discovery that using the thruster in a small vacuum vessel requires minor modification of the tuner adjustments from the settings appropriate when the thruster is used in wider tank or in free space. Surprisingly, the simulations indicated that the cross talk between the applicator was not significant as long as both cavities are powered simultaneously and that the tuner settings for the ionization and acceleration applicator systems are similar. These unexpected results point to the major drawback of the method employed: simulation cannot really integrate realistic resonant inhomogeneous plasma behavior. Nevertheless, the applicators developed are sufficiently versatile to be tuned to resonance even when loaded with strongly perturbative plasma and to allow measuring such plasma impedances'.

B. Magnetic Structure Design Development.

We will now review the principles that have influenced our efforts in designing the magnetic structure for the electrodeless plasma thruster and a few of the resulting magnetic field structure.

The magnetic field plays three critical roles in the electrodeless plasma thrusters:

- Creating a resonant magnetic field surrounded by a "magnetic bottle" for the ionization stage
- Creating a decreasing magnetic field around another resonant value to produce the magnetized ponderomotive force field.
- Confining the plasma away from the thruster structure

The simplest magnetic structure able to produce a field fulfilling these three requirements is simply composed of two coils surrounding and spaced along the thruster axis. Such a structure resemble to a Helmholtz Coils setting in which would be voluntarily spaced further away than their diameter to produce an area of lower magnetic field intensity between them (Fig. 18). Of course, this basic design can be fitted with additional coils to finely adjust the magnetic field profile along the thruster chamber (Fig. 19).

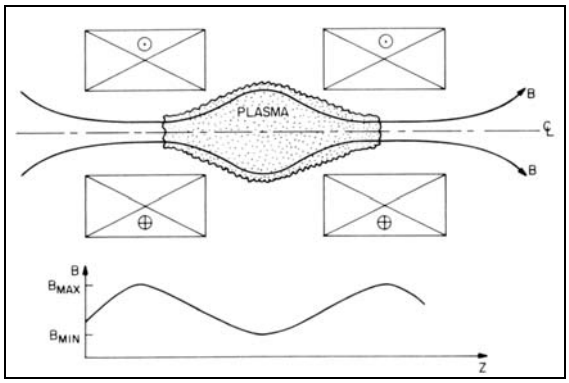

Figure 18. Simplest coil arrangement. *The magnetic field lines clearly exhibit the magnetic bottle feature between the coils confirmed by the inset magnetic field intensity plotted below against the axial position. This example expose symmetric*

Nevertheless, this configuration suffers from important drawbacks: coils are large, heavy, requires additional DC current sources and create heat loads. Last the power used to create the magnetic field with the coils actually create an extended fringing magnetic field outside the thruster itself which is inefficient and can even require additional magnetic shielding to protect other spacecraft components. Incidentally, all these problems become substantial when trying to create field intensity resonant with 2.45 GHz on a volume of approximately 600 cm^3.

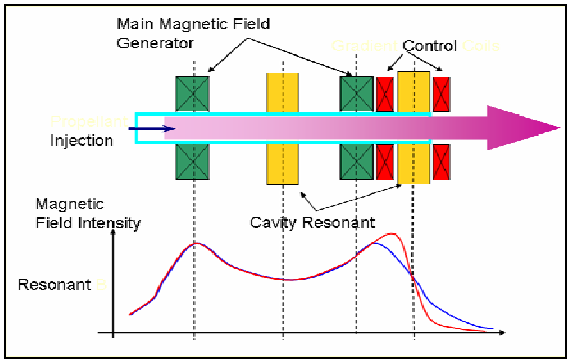

Figure 19. Overview of an advanced coil-based magnetic structure. *The magnetic field intensity along the thruster chamber can be modified from the blue cure to the red curve by modifying the current in the control coils (Red Coils) located around the acceleration applicator.*

Hence, there is a strong interest of creating alternative magnetic field assembly relying on permanent magnet or electromagnet instead of only coils.

Simple magnetic bottle can be produced using either of them as illustrated in Fig. 20. The only difference being that the magnetic field lines now, after being compressed in area of high magnetic field intensity, close on the magnetic structure itself. This could pose a problem as energetic electrons, which are bound to the magnetic field line, might impinge on the magnetic structure at these spot and create localized heat load. Yet, the particle and power flux on these surfaces can be strongly reduced as the absolute field intensity becomes larger. Indeed, the strong gradient creates an intense magnetic mirror effect.

One of the first improvement over fully coil-based structure can be described as a hybrid structure using a permanent magnet assembly produce a simple axial decreasing magnetic field that is modified to form magnetic bottle by using only one additional coil (Fig. 21). In these scheme the required coil current can be reduce by 50% to 90% and the coil mass by 20% to 40%. This design has the advantage that the field line presents no cusp inside the thruster chamber.

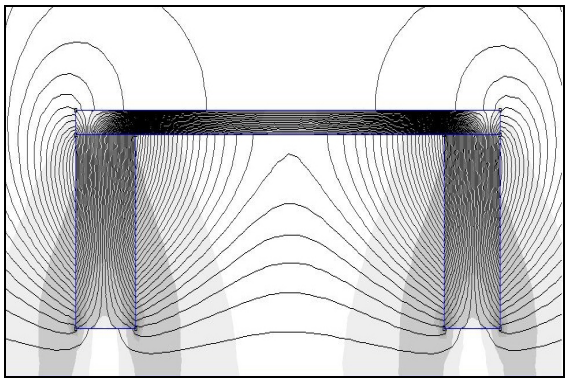

Figure 20. Overview of magnetic field line created by a U-shape magnet. *The magnetic field intensity is presented by grey density. The field line between the pole pieces form simple magnetic bottle.*

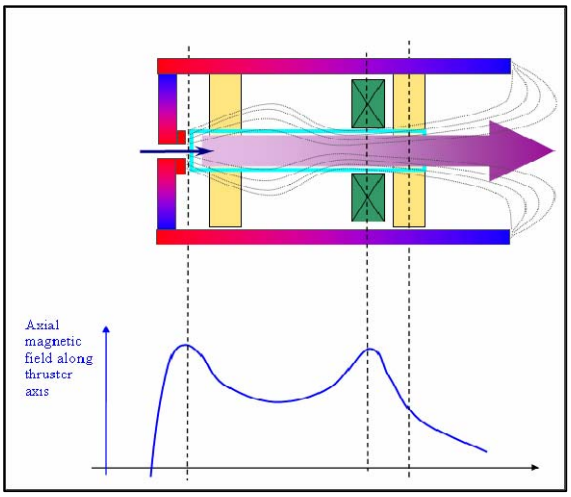

Figure 21. Overview of a hybrid magnetic structure. *The magnetic field lines are schematically represented by dotted line. Red & blue colored element represent magnets with North Pole indicated in Red. Grey parts represent high permeability elements*

A further step consists in using only magnets; two possible magnet-based structures are represented in Fig. 22 and Fig. 23. The structure can be created by using a set of radially oriented cylindrical magnets, or using axially magnetized rod magnets, with high permeability elements (flanges and/or rods). These structures create both a magnetic bottle around the ionization stage and a suitable decreasing field in the acceleration stage. On the other hand, the magnetic field lines present a cusp between the two stages where the plasma behavior can create problematic particle impact flux on the structure despite the potent radial magnetic mirror effect.

However, using a proper set of diversely oriented magnets, our team conceived magnetic assemblies such that no cusps are present inside the thruster chamber. In fact, the cusp areas are rejected off-axis and surround the thruster chamber where they do not affect plasma behavior. Figure 24 present the magnetic field created by one of these complex magnet assembly. This field clearly fulfills the thruster requirements. One noticeable characteristic of this structure is the ability to adjust the exact position of the resonance area by a small change in the respective position of some magnets.

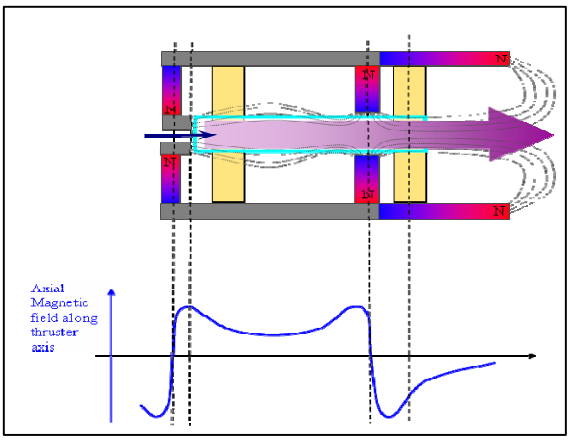

Figure 22. Overview of an advanced permanent magnet assembly. *The magnetic field generates a bottle around the ionization applicator and a decreasing field in the acceleration stage. The magnetic cusp between these stages is clearly visible.*

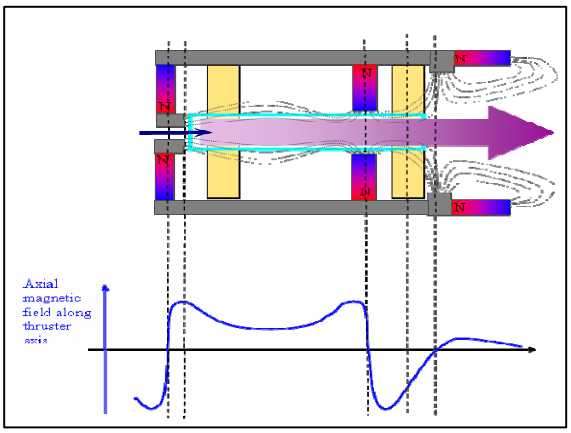

Figure 23. Overview of an advanced permanent magnet assembly. *This arrangement allows greater control over the decreasing magnetic field in the acceleration stage.*

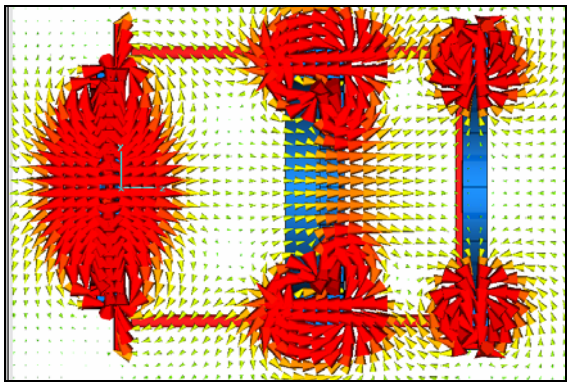

Figure 24. Overview of the magnetic field produced by an advanced permanent magnet assembly in the vertical plane. *The magnetic bottle structure and magnetic field line continuity from the ionization to the acceleration stage are apparent. Two off-axis cusps are visible outside the plasma chamber.*

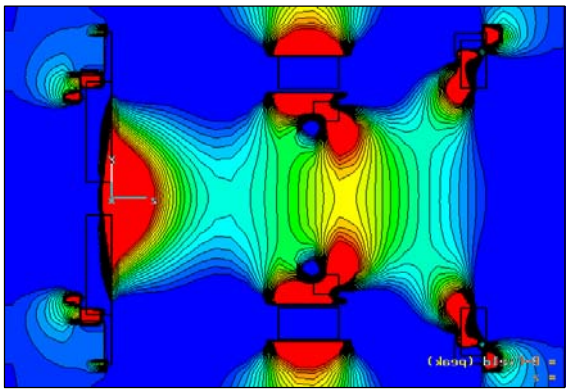

Figure 25. Overview of the axial magnetic field intensity produced by an advanced permanent magnet assembly in the vertical plane. *Red color shows high axial magnetic field intensity whereas blue are show are of negative axial field. The magnetic bottle structure clearly appears as the yellow area in the center of the image.*

Figure 25 confirms that the magnetic field behavior satisfy all the requirements. Incidentally, the agreement between the magnetic field computed by finite elements model and experimentally measured on the actual structure is stunning. The discrepancies were smaller than the measurement uncertainty (see Fig. 26 & Fig. 27).

This magnetic structure relies on magnets of unusual size and magnetization state, thus seemed to have never been produced before[**]. These powerful and large magnets apply intense mechanical force on the structure, reaching more than 2000 N on some components. This structure also holds more pleasant characteristics such as producing very limited fringing magnetic field, making them easier to integrate on a spacecraft.

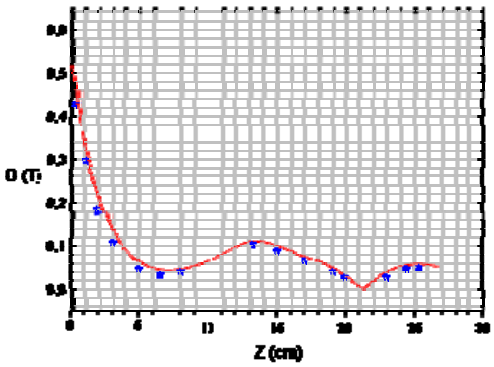

Figure 26. Axial magnetic field intensity along the thruster axis. *The red curve is the results of FEA simulation. The blue dots are experimental measurements. The measurement uncertainty (+/- 5mT) is larger than all difference between the measurement and calculated value.*

Figure 27. Magnetic field structure on magnetic field measurement bench. *The structure axis is set vertically. The Hall Effect probe can be seen in the acceleration stage area.*

[**] Please refer to the acknowledgment section,

IV. High Power Electrodeless Plasma Thruster Prototype

The high power electrodeless plasma thruster prototype (Fig. 28) use advanced microwave applicator systems and advanced magnetic assembly. These advanced systems allow using this prototype to investigate experimentally the dynamics of the microwave-plasma coupling both in the ionization stage and in the acceleration stage.

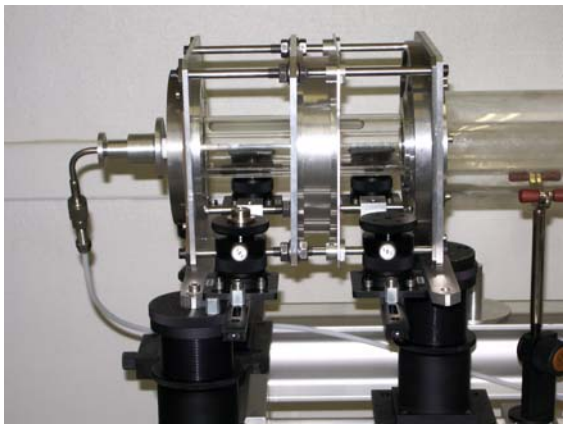

Figure 28. High power electrodeless plasma thruster prototype. *The propellant injection system appears on the right. Microwave applicators have been removed. The glass tube on the right is a small vacuum vessel.*

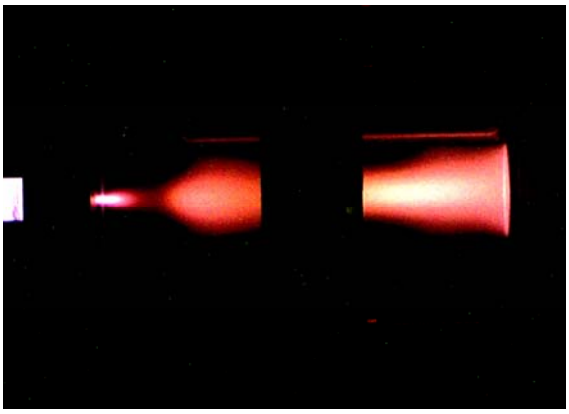

Figure 29. Plasma beam inside the high power electrodeless plasma thruster prototype during tests. *The plasma beam shape follows the magnetic field line shape. The dark area in the middle of the thruster length is the shadow a magnetic component.*

The information gathered from these experimental investigations of the microwave-plasma coupling, will allow our team to design a broad variety of optimized thruster adapted to specific mission requirements.

Acknowledgments

The Elwing Company wishes to express its gratefulness to all the specialist partners: SAIREM SA, Swift-Levick Arnold Magnetics Ltd and Façon Mécanique SARL, which have all assisted our team during this long development phase. Precisely, one author, Gregory Emsellem is glad to acknowledge the outstanding contribution of Dr. Jean-François Rochas and Dr. Jean-Marie Jacomino who patiently guided us in the subtle, and unintuitive, realm of microwave design. Similarly, the contribution of Dr. Ewan Goodier and Dr. Ken Ball and their colleagues, who strived to successfully manufacture and assemble the challenging magnet assembly components.

Besides, Gregory Emsellem would like to state here his deep gratitude to Dr Richard Geller, for his kind assistance, erudite advices and heart-lifting enthusiasm for a new application of ECR.

Last, the Elwing Company wants to thanks our investors for their steadfast commitment and earnest support.

References

[1]Michel Moissan & Jacques Pelletier, editors, *Microwave excited Plasmas*, Elsevier Science Publishers B.V., Amsterdam, 1992

[2] Richard Geller, *Electron Cyclotron Resonance Ion Sources and ECR Plasmas*, IOP Publishing Ltd., Bristol, 1996

[3] Tse V. Chow Ting Chan & Howard C. Reader, *Understanding microwave heating cavities*, Artech House, Boston, MA, 2000.